Fermilab FERMILAB-Conf-06-244-AD July 2006

Superconducting Magnets in High-Radiation Environment at Supercolliders*

N.V. Mokhov, D.R. Chichili (FNAL, Batavia, IL)†
S.A. Gourlay (LBNL, Berkeley, CA)
S. Van Sciver (NHMFL, Tallahassee, FL)
A. Zeller (NSCL, East Lansing, MI)

July 17, 2006

Abstract

The principal challenges arising from beam-induced energy deposition in superconducting (SC) magnets at high-energy high-luminosity hadron and lepton colliders are described. Radiation constraints are analyzed that include quench stability, dynamic heat loads on the cryogenic system, radiation damage limiting the component lifetime, and residual dose rates related to hands-on maintenance. These issues are especially challenging for the interaction regions (IR), particularly for the considered upgrade layouts of the Large Hadron Collider. Up to a few kW of beam power can dissipate in a single SC magnet, and a local peak power density can substantially exceed the quench levels. Just formally, the magnet lifetime is limited to a few months under these conditions. Possible solutions and the ways to mitigate these problems are described in this paper along with R&D needed.

*Presented paper at the *Super Magnets for Supercolliders Workshop*, Erice, Sicily, October 26 - November 1, 2003

†Work supported in part by the Universities Research Association, Inc., under contract DE-AC02-76CH03000 with the U. S. Department of Energy

1 Introduction

The Large Hadron Collider (LHC) under construction at CERN will produce pp collisions at $\sqrt{s}$=14 TeV and luminosity $\mathcal{L}$=10^{34} cm^{-2}s^{-1}. The interaction rate of 8×10^8 s^{-1} represents a power of almost 900 W per beam at each Interaction Point (IP), the majority of which is directed towards the low-β insertions in the form of the collision byproducts, with about one third of the power carried out by neutrals in the very forward direction [1]. At future supercolliders under consideration – various LHC upgrade scenarios first of all [2, 3] – the IP power is up to a factor of ten higher. The quadrupole or dipole fields sweep the secondary particles into the coils along the vertical and horizontal planes, giving rise to a local peak power density ε_{max} that can substantially exceed the quench limits. Corresponding dynamic heat load can exceed the cryogenics capacity. Build-up of radiation defects can drastically reduce component lifetime. Hands-on maintenance is rather difficult if all components in the entire region are highly radioactive. The corresponding IR layout, magnet design and materials, and an appropriate set of collimators and absorbers must provide adequate mitigation of these problems.

Contrary to the IR magnets, the majority of the main ring SC magnets are in rather "comfortable" conditions with an adequate, highly-efficient, collimation system. The concerns here are a cryoplant capability and accidental beam loss of GJoule beams with a possible destruction of machine components.

In both cases, a lack of data on radiation limits for materials used in the SC magnets – especially in high-energy domain – makes the radiation damage and component lifetime situation at supercolliders rather uncertain.

2 Radiation Sources at Supercolliders

There are three radiation sources in a collider with dose D in the SC coils proportional to the luminosity $\mathcal{L}$ or beam loss power $Q\times\Delta I$:

1. pp collisions: $D\sim\sigma_p\times\mathcal{L}$, where σ_p is a corresponding non-elastic cross section.
2. Operational beam loss: tails from collimators and beam-gas scattering, $D\sim Q\times\Delta I$, where Q is total beam energy, and ΔI is beam loss rate.
3. Accidental beam loss: abort kicker prefire / unsynchronized beam abort, $D\sim Q\times\Delta I$.

Table 1 compares, relevant to this report, parameters of the hadron colliders: existing Tevatron, LHC under construction at CERN, "modest" and "ultimate" LHC upgrades, LHC-2 and SLHC, respectively [4], and two stages of a Very Large Hadron Collider, VLHC-1 and VLHC-2 [5]. The LHC rule was used to calculate a number of non-elastic interactions N_{10} at each IP over 10 years of operation: $\mathcal{L}_{10yr}$ = (0.1+1/3+2/3+7) $\times\mathcal{L}$ at 180 days/yr. 10 yrs = 5×10^7 s $\rightarrow$ 500 fb^{-1}. The interaction rate 8×10^8 int/s at σ_p=80 mb and $\mathcal{L}$=10^{34} cm^{-2}s^{-1} give N_{10} = 4×10^{16} int/10 yr.

A power of up to 1 to 10 kW per beam is directed towards the low-β insertions on either side of each IP causing severe short- and long-term radiation problems described above. Only with appropriate IR layout and magnet design [3], use of radiation-resistant materials and highly efficient protection system [1], one can provide reliable operation of these machines.

As for accidental beam loss, it was shown in Refs. [6, 7] that at an unsynchronized beam abort in the LHC, up to 10% of total beam power Q can end up in the IR – which can literally explode one or two quadrupoles and expensive detector components – if not intercepted in the beam abort section by a highly sophisticated protection system. This case is out of scope of this paper.

Table 1: Particle energy E, beam intensity I (ppp), their product Q, collision energy $\sqrt{S}$, luminosity $\mathcal{L}$, and a of non-elastic interactions at IPs over 10 years of operation N_{10} at hadron colliders.

Machine	E (TeV)	I, 10^{14}	Q (GJ)	$\sqrt{S}$	$\mathcal{L}$, 10^{34}	N_{10}, 10^{16}
Tevatron	0.98	0.1	0.0016	1.96	0.01	
LHC	7	3.1	0.35	14	1	4
LHC-2	7	4.8	0.54	14	2.5	10
SLHC	7	9.6	1.08	14	10	40
VLHC-1	20	9.7	3.20	40	1	4.5
VLHC-2	100	2.0	3.20	200	2	10.5

3 Protection System in IR

At the LHC, after thorough optimization of the IR layout, an IR protection system was designed to protect SC magnets against debris generated in the pp collisions and in the near beam elements [1]. The optimization study was based on detailed energy deposition calculations with the MARS code [8]. The system includes a set of absorbers in front of the inner triplet, inside the triplet aperture and between the low-β quadrupoles, inside the cryostats, in front of the D2 separation dipole and between the outer triplet quadrupoles. Their parameters were optimized over the years via the MARS runs to provide better protection and to meet practical requirements at the same time.

Fig. 1 shows the inner triplet configuration. The two curves show the approximate "n1 = 7" (number of beam σ's) beam envelope for injection and collision optics, including closed orbit and mechanical tolerances [1].

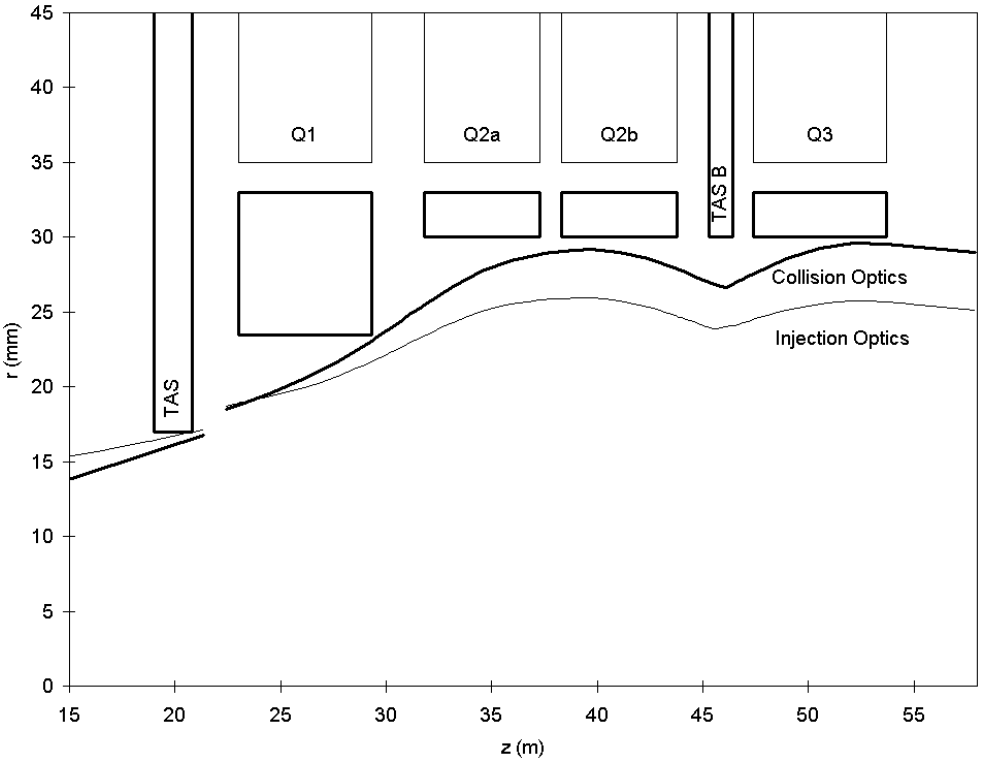

Figure 1: The LHC low-β insertions including absorbers: schematic view with the beam envelopes.

The following design constraints are put on the IR protection system [1]:

1. Use ultimate design luminosity: 10^{34} cm^{-2}s^{-1} at LHC through 10^{35} cm^{-2}s^{-1} at SLHC.
2. Geometrical aperture: keep it larger than "n1 = 7" for injection and collision optics, including closed orbit and mechanical tolerances.
3. Quench stability: keep peak power density ε_{max}, which can be as much as an order of magnitude larger than the azimuthal average, below the quench limit with a safety margin of a factor of 3.
4. Radiation damage: with the above levels, the estimated lifetime exceeds 7 years even in the hottest spots.
5. Quench limit: tests of porous cable insulation systems and recent calculations concerning the insulation system to be used in the Fermilab-built LHC IR quadrupoles (MQXB) have shown that up to about 1.6 mW/g can be removed while keeping the coil below the magnet quench temperature.
6. Dynamic heat load: keep it below 10 W/m.
7. Hands-on maintenance: keep residual dose rates on the component outer surfaces below 0.1 mSv/hr.
8. Engineering constraints must always be obeyed.

As a result of optimization of the protection system, it became possible to meet these constraints for the LHC IR at the design luminosity of 10^{34} cm^{-2}s^{-1}, with $\varepsilon_{max} \leq 0.45$ mW/g. Note that the power density in the SC coils always peaks in the horizontal or vertical planes at the coil inner-most radius.

4 LHC Upgrades and Beyond

After the LHC operates for several years at a nominal luminosity $\mathcal{L} = 10^{34}$ cm^{-2} s^{-1}, it will be necessary to upgrade it for higher luminosity. In a traditional quadrupole-first design, ε_{max} and other energy deposition values grow proportionally to the luminosity, and in general increase with the quadrupole length and gradient and decrease with aperture. It was shown [3] that this option is viable at modest $\mathcal{L}$ upgrades up to about 2.5×10^{34} cm^{-2} s^{-1}.

At higher luminosities, the most attractive option is a double-bore inner triplet with separation dipoles placed in front of the quadrupoles [2]. Compared with the baseline design consisting of single-bore quadrupoles shared by both beams, this layout substantially reduces the number of long-range beam-beam collisions, allows the beams to pass on-axis through the quadrupoles, and permits local correction of triplet field errors for each beam. Increasing the LHC luminosity by an order of magnitude creates a hostile radiation environment resulting from colliding beam interactions.

The problem is particularly severe for the dipole-first layout, since most of the charged secondaries will be swept into the dipole by its large magnetic field. Detailed MARS energy deposition calculations have been performed to determine the feasibility of this approach [9]. Fig. 2 shows the layout considered. The D1 dipole starts at 23 m, allowing space, as in the current IR, for a 1.8-m long TAS absorber, and there are 5 m between the D1 and D2 to allow for a TAN neutral particle absorber. The orbits shown are for a horizontal crossing angle of $\pm$0.212 mrad.

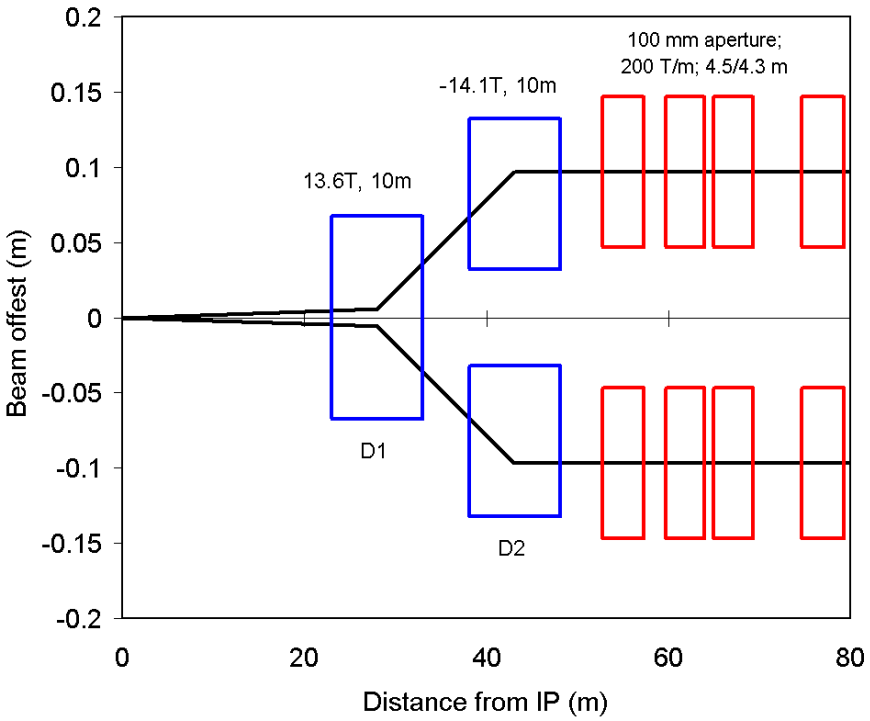

Figure 2: Dipole-first interaction region layout.

The studies are done for the SLHC D1 of two types: a traditional cos-theta design with a 4-layer graded coil of inner radius 65 mm and a cold iron yoke, and an open mid-plane block type coils. At $\mathcal{L} = 10^{35}$ cm^{-2} s^{-1}, the total power dissipated in the dipole is about 3.5 kW in either design. ε_{max} in the cos-theta coils reaches 50 mW/g, almost two orders of magnitude higher than in the baseline LHC optics. It can be reduced to about 13 mW/g with some spacers in the mid-plane, being still unacceptably high. The fact that the radiation peaks in the mid-plane, has spurred the design of an open mid-plane dipole magnet [9]. Tungsten rods at liquid nitrogen temperature are placed in the mid-plane to absorb much of the radiation. Fig. 3 shows power density profiles in such a dipole at the longitudinal maximum at its non-IP end. Peak power density ε_{max} in the coils of the block-type dipole with no material on the mid-plane can be reduced well below the quench limit. More than a half of the total heat load can be absorbed in the rods at high temperatures. Efficient removal of remaining power from the cryogenic system is a major challenge for implementing this IR design as part of an LHC upgrade. It must be emphasized that such a design has never been tried, and substantial R&D must be done before the feasibility of a magnet of this type can be demonstrated.

Table 2 shows the peak dose and neutron fluence in the supercollider IR SC coils at the hottest spots: Q2B quadrupole at β_{max} in a quadrupole-first traditional layout (LHC, LHC-2, VLHC-1 and VLHC-2), and D1 in the dipole-first configuration (SLHC). It is useful to note that D (MGy/yr) = 50 ε (mW/g). This table is the input for the material lifetime analysis in the next section.

Dynamic heat loads in the LHC high-luminosity IRs on either side of IP at $\mathcal{L} = 10^{34}$ cm^{-2} s^{-1} are rather high [1]. At cryo temperatures these are about 30 W in each of the four quadrupoles totaling 114 W, 19 W in corrector magnets and feedbox, 2 W in the D2 separation dipole, and 0.5 to 2 W in the outer triplet quadrupoles. At room temperature, the main players are 184 W in the front absorber TAS, 6 W in intermediate absorbers, 50 W in the D1 separation dipole, and 189 in the neutral beam absorber TAN. These numbers scale up with the luminosity.

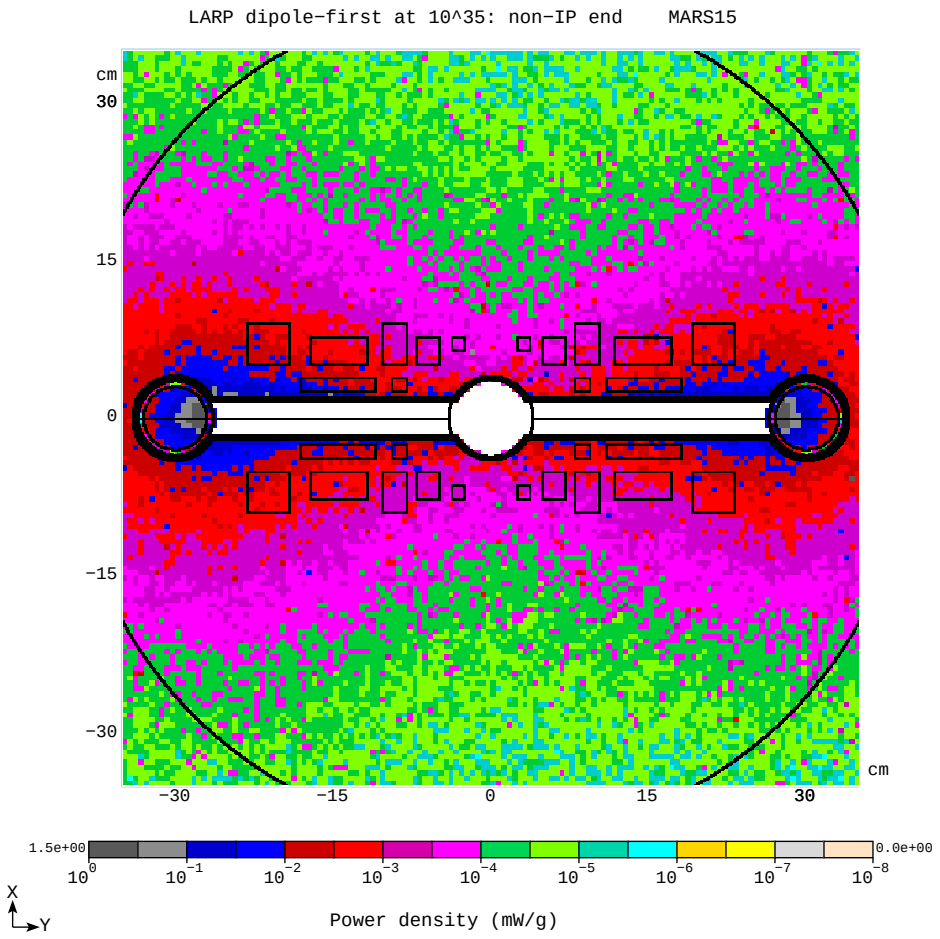

Figure 3: Power density isocontours in the open mid-plane dipole.

Table 2: Peak dose D and neutron fluence $F_{>0.1\ MeV}$ in inner triplet SC coils accumulated over first 10 "LHC" years (=5×10^7 sec).

Machine	Component	D (MGy)	$F_{>0.1\ MeV}$, 10^{16} cm^{-2}
LHC	Quad Q2B	22.5	1.04
LHC-2	Quad Q2B	45.0	2.08
SLHC	Cosθ D1	650	30
SLHC	Block coil D1	55.0	2.54
VLHC-1	Quad Q2B	∼30	∼1.5
VLHC-2	Quad Q2B	∼84	∼4

Residual dose rates are quite significant in the near beam region [1]. At $\mathcal{L} = 10^{34}$ cm^{-2} s^{-1}, after 30-day irradiation and 1-day cooling they are up to several hundred mSv/hr at the TAS front absorber and Q1 thick beam tube, up to several tens mSv/hr at the inner parts of the quadrupoles, and below 0.1-0.3 mSv/hr on contact at the outer vacuum vessel at r∼45 cm. These numbers also scale up with the luminosity.

5 Material Lifetime

Magnets are composed of superconductor (Nb_3Sn), copper, insulation and structural materials (stainless steel or equivalent). All of these materials have different radiation sensitivities and responses to radiation damage. Additionally, the sensitivities and responses are temperature dependent.

5.1 Material limits

The limits for Nb_3Sn depend on the particular application. All three critical components of the superconducting phase space (T_c, I_c and B_{c2}) are reduced by different amount for a given radiation dose. Some general limits [10] are:

- T_c goes to 5 K for 5×10^{19} n/cm^2.
- I_c goes to 0.9 I_{c0} at 1×10^{19} n/cm^2 (at 14 T).
- B_{c2} goes to 14 T at 3×10^{18} n/cm^2.

From this we see that B_{c2} is the most sensitive parameter and would be the determining factor at a dose where the critical current is largely unaltered. Fortunately, at supercolliders the neutron fluence is low enough that this isn't of too much concern; although the higher energy neutrons in the accelerator are more damaging than the reactor-spectrum used to derive the above limits, so the problem cannot be ignored.

Of more concern is the copper stabilizer increasing in resistance with dose. Since the protection depends on the copper as a low resistance parallel path and the stability on the excellent thermal conductivity, reductions in these properties put the magnets at risk. Most of the increased resistance can be annealed out by warming to room temperature, but this puts the machine down for the thermal cycle. Note, however, that Nb_3Sn annealing requires warming to 900 K, so would not be useful for complete magnets.

It also poses an additional risk: Radiation resistant epoxies, such as cyanate esters, produce gas as hydrogen is formed by the radiation (neutrons or photons). This gas is immobile at 4 K but expands if the magnet is warmed up. Cracking of the epoxy is an obvious risk, as well as loss of integrity, every time the magnet is thermally cycled. Even if epoxies are not used and radiation tolerant ceramics are used instead, there is still a potential problem. Ceramics, such as BeO, exhibit a linear expansion with radiation dose. Alumina, however, shrinks with radiation. This will change the preload on the coil over time and thermal cycle.

Other structural materials, such as stainless steel, become brittle with very high energy deposition. Generally, this is of less concern because of very high doses required for damage thresholds.

General radiation dose limits are given in Table 3. The limits are derived from the material properties that are the most sensitive.

Table 3: General radiation dose limits.

Material	Useful limit (MGy)
Copper	$> 10^4$
Iron, Stainless steel	$> 10^4$
Ceramic	$> 10^3$
Organics	$\sim 10^2$

5.2 R&D Needed

1. Detailed calculations of the local radiation fields at sensitive points that correspond to places of high magnetic field and high shear stress. Radiation damage is akin to high magnetic field in that the place with the highest damage determines the lifetime, just as the highest magnetic field determines performance.

2. Data at neutron energies greater than 14 MeV. Reactor data is the most abundant and easiest to obtain and some way of relating that to the higher energy neutrons that predominate the spectra at accelerators is required.

3. Damage studies on the newest Nb_3Sn materials. Most of the data are 15-20 years old and there have been significant advances in the last few years. The responses of the newer materials to radiation are unknown.

6 Thermal Analysis

Thermal analyses of the proposed designs for LHC-2 IR quadrupole [11, 12, 13] and SLHC dipole-first magnet [9, 14] have been performed to get an idea of the peak temperatures in the coil due to radiation heat loads and magnet operation margins. The following two sub-sections summarize these results.

6.1 LHC-2 IR quadrupole

The proposed LHC-2 IR quadrupole magnet is based on a two-layer cos-2θ design with Nb_3Sn conductor and 90-mm bore diameter. The total number of turns is 144 with coil area of 48.1 cm^2. MARS-calculated power density were applied on the coil geometry as a function of radius and angle [1, 12, 15]. As mentioned in previous sections, the power density peaks at the inner layer of the mid-plane turns. It decreases with increase in radius and angle. Fig. 4 shows the comparative power density in the mid-plane turns for the current LHC IR quads and proposed LHC-2 quadrupole. At $\mathcal{L} = 10^{35}$ cm^{-2} s^{-1}, the expected radiation loads are an order of magnitude larger for quadrupoles compared to that of the baseline LHC design.

Based on these heat loads, peak temperature was first computed from ANSYS analysis. The peak temperature was then converted into the operating margin based on the superconductor transport properties. Based on this analysis, it was noted [12, 13] that Nb_3Sn magnet designed with a 20% quench margin can take up to 40 mW/cm^3 of peak power density in the coil mid-plane turns at the operation temperature of 1.9 K.

6.2 SLHC dipole-first

One of the two SLHC separation dipole-first magnets considered in Ref. [9] is based on a four-layer cos-theta design with a bore diameter of 130 mm. It is placed in front of the IR triplet region. Total number of turns is 282 with coil area of 119.1 cm^2. The magnetic field at quench in the bore is 15.8 T for J_c (12 T, 4.2 K) = 3000 A/mm^2. Heat deposition distribution in the coil was calculated with the MARS code and applied on the coil elements. A copper spacer would be inserted in the mid-plane to reduce the heat load to superconductor. As mentioned in previous sections, the peak power density in the copper spacer is 49 mW/g and that in the coil is 13 mW/g.

A thermal analyses for this design were performed in Ref. [14] with different boundary conditions. Table 4 summarizes these results. The thermal calculations were based on cooling conditions

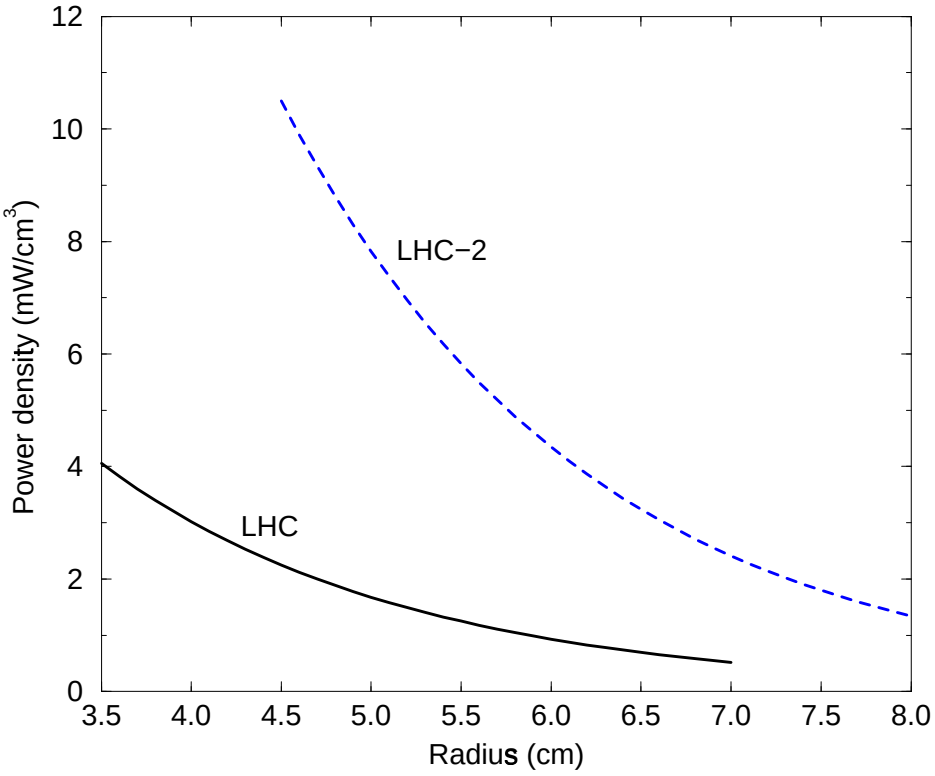

Figure 4: Radial distribution of power density in the mid-plane turns for the LHC and LHC-2 IR quadrupoles at longitudinal maxima.

that set the coil perimeter at 1.9 K. Cooling inner coil surface with perforated insulation in addition to external, inter-layer and mid-plane cooling seems to be the way to manage the temperature rise due to radiation heat loads.

Table 4: Peak temperature T_{max} in cos-theta SC coils of SLHC dipole-first.

Cooling conditions	T_{max} K
Coil (external) surface 1.9 K	27.7
Coil (external + mid-plane) surfaces 1.9 K	24.8
Coil (external + inter-layer) surfaces 1.9 K	11.3
Coil (external + inter-layer + mid-plane) surfaces 1.9 K	11.3
Porous inner bore + All the above	7.0

7 Cryogenic Considerations for Dipole-First

Current designs for the upgraded dipole magnets in the interaction regions indicate a very high heat load from the radiation environment. As discussed in previous sections, this high radiation environment will impact the lifetime of materials contained in the magnets potentially requiring innovative design concepts and new materials. In addition, this heat deposition can lead to large thermal gradients within the magnet structure affecting magnet performance. Ultimately, all the

radiation flux deposited heat in the magnets that must be removed by the cryoplants. In the case of upgrades to LHC, this issue is of concern given the magnitude of the heat deposition compared to current LHC operating parameters. Clearly an upgrade to the cryoplants will be required for any of the planned upgrades.

The SLHC luminosity upgrade dipole-first design predicts a 3.5 kW heat load per 10 m IR region dipole. Since the accelerator has four such regions, the total low-temperature heat load associated with these IR magnets is 14 kW at low temperature. This heat load alone is comparable to the total current LHC accelerator magnet cooling load. The installed cryogenic system for the LHC is divided into eight sectors, each supported by a nominal 18 kW at 4.5 K refrigerator. These machines supply 30 kW between 50 and 75 K for shield cooling, 5 to 6 kW between 4.5 and 20 K for beam screen cooling and 2.4 kW at 1.9 K for magnet cooling [16, 17]. Thus, for the entire accelerator, there is approximately 40 kW of refrigeration for the beam screens and 19.2 kW at 1.9 K for magnet cooling.

In steady operation with the present LHC magnet and cryostat design, the 1.9 K heat load from the accelerator magnets has an average value of less than 0.4 W/m corresponding to 10.8 kW or roughly half the total 1.9 K capacity of the cryogenic system. In each interaction region, the current heat load is 110 W for four quadrupole magnets, a factor of 30 less than calculated for the dipole-first design. The additional 1.9 K capacity is used for off-normal operation.

Any upgrade of the LHC operation will result in an increase in the heat load to the cryogenic plant. A luminosity upgrade from 10^{34} to 10^{35} cm^{-2} s^{-1}, will result in increase in beam screen heat load from 1.7 W/m to 15 W/m for a total heat load between 4.5 and 20 K of over 400 kW [18]. It also possible that the higher luminosity will increase the steady heat load on the accelerator magnets, but this impact is not known at the present time. Clearly, the current cryogenic plant is insufficient to meet this requirement.

Use of a high radiation absorbing dipole in the interaction region of the upgraded LHC will also severely impact the cryogenic system. According to the design, each dipole-first will absorb 3.5 kW of radiation heat during normal operation, resulting in a total impact on the accelerator of 14 kW over these localized regions. In addition to the impact on the total heat load to the cryoplant, careful consideration to the magnet and cryostat design will be needed to ensure stability and reliable operation. For example, it may be necessary to consider alternate cooling technologies to 1.9 K, pressurized He-II bath cooling for the dipole-first. This point is further emphasized as indicated in the previous section, by the calculations that indicate the temperature within the magnets may exceed 20 K even if cooled with He-II at 1.9 K. Clearly this temperature is too high for conventional magnet design using NbTi or even Nb_3Sn superconductor.

Innovative magnet and cooling systems design may reduce the peak temperature of the dipole to the point where one could consider using Nb_3Sn superconductor at 1.9 K. However, the cost of operating such magnets may be too large a penalty for the cryogenic plant. Alternatively, it may be possible to use more recently developed ceramic superconductors operating around 20 K. The higher operating temperature would reduce the equivalent refrigeration power by roughly a factor of ten. To consider this option, further research would be needed to determine the resistance of these materials to radiation damage.

8 Summary

With careful design of IR layout, magnets and protection system, we can keep a peak power density ε_{max} below the quench limit:

- in 90-mm 200-T/m Nb_3Sn quads at $\mathcal{L} \leq 2.5\times10^{34}$ with 30 W/m of dynamic heat load at peak (compared to 10 W/m now) in LHC;
- in a 14-T Nb_3Sn dipole-first D1 at $\mathcal{L} \leq 1\times10^{35}$ with total power dissipated in the dipole of about 3.5 kW, with a superconductor-less mid-plane design.

A $\sigma_p \times \mathcal{L}$ scaling gives a reasonable estimate for supercollider IRs, although details of spatial distributions can be obtained via realistic Monte Carlo. It turns out that there is no strong dependence of peak power density ε_{max} on the coil aperture because one needs to adjust the gradient appropriately. Rules of thumb here are:

- at fixed aperture, the stronger field the higher ε_{max};
- at fixed field, the larger aperture the lower peak ε_{max} with heat load distributed more uniformly along the triplet with more secondaries (power) leaking towards its end and further (TAN and outer triplet).

Dynamic heat load is a serious issue. All radiation issues are very serious at higher luminosities. The design is below the quench limit for Nb_3Sn, but is a factor of 2 to 3 times larger than for current NbTi quadrupoles. Accumulated dose, residual dose rates and other radiation values inside and outside magnets scale up with luminosity, linearly to the first approach. With the present design, at $\mathcal{L} = 10^{34}$, we are on a 7-year limit for material lifetime and on or above the CERN limits for residual radiation. Much more MARS analysis is needed here on configuration and materials.

Operational and accidental beam loss in the inner and outer triplets is a serious issue, with their higher magnetic fields. The results we have for the current design are already somewhat scary. We have a sophisticated monstrous movable collimator in IP6 to handle unsynchronized beam abort, but it seems that to reliably protect IP5 inner triplet we would still need another collimator on the non-IP side of the current D1. At SLHC everything becomes more severe.

TAS itself and shielding around TAS-Q1 need to be re-designed to suppress ten times (at least) higher albedo fluxes to ATLAS and CMS-like detectors. Neutral beam absorber TAN and its shielding need to be re-designed to accommodate ten times higher beam power and provide adequate shielding for prompt and residual radiation.

Work needed:

- Further characterize various IR designs in terms of radiation environment, with respect to peak energy deposition, fluence, dose, and cryo load.
- Define material properties and acceptable design criteria for given dose
- Survey fusion program results: identify relevant information and identify areas for focus (Nb_3Sn behavior in LHC IR radiation field).
- Develop appropriate tests (materials, magnetization tests in lieu of direct J_c, etc).
- Identify existing rad hard materials for incorporation into magnet programs.
- Focus R&D on what is left.

References

[1] N.V. Mokhov, I.L. Rakhno, J.S. Kerby, J.B. Strait, "Protecting LHC IP1/IP5 Components Against Radiation Resulting from Colliding Beam Interactions," Fermilab-FN-732 (2003), LHC Project Report 633 (2003).

[2] J.B. Strait, et al., "Towards a New LHC Interaction Region Design for a Luminosity Upgrade", PAC2003 Proc., p. 42; Fermilab-Conf-03/098 (2003), LHC Project Report 643 (2003).

[3] J.B. Strait, N.V. Mokhov, T. Sen, "Overview of Possible LHC IR Upgrade Layouts", Fermilab-Conf-05/007-AD-E-T (2005).

[4] O.S. Brüning et al., "LHC Luminosity and Energy Upgrade: A Feasibility Study," LHC Project Report 626 (2002).

[5] "Design Study for a Staged Very Large Hadron Collider", Ed. H.D. Glass et al., Fermilab-TM-2149 (2001).

[6] A.I. Drozhdin, N.V. Mokhov, M. Huhtinen, PAC1999 Proc., p. 1231 (1999).

[7] N.V. Mokhov, A.I. Drozhdin, I.L. Rakhno et al., PAC2001 Proc., p. 3168 (2001).

[8] N.V. Mokhov, "The MARS Code System User's Guide," Fermilab-FN-628 (1995); N.V. Mokhov, "Status of MARS Code," Fermilab-Conf-03/053 (2003).

[9] N.V. Mokhov, et al., "Energy Deposition Limits in a Nb_3Sn Separation Dipole in Front of the LHC High-Luminosity Inner Triplet", PAC2003 Proc., p. 1748; Fermilab-Conf-03/083 (2003), LHC Project Report 646 (2003).

[10] N.J. Simon, "Radiation Limits for Nb_3Sn Superconductors for ITER Magnets", NIST report (1995).

[11] A.V. Zlobin et al., "Conceptual Design Study of Nb_3Sn Low-beta Quadrupoles for 2nd Generation LHC IRs", *IEEE Transactions on Applied Superconductivity,* v. 13, No. 2, p. 1266 (2003).

[12] A.V. Zlobin et al., "Large-Aperture Nb_3Sn Quadrupoles for 2nd Generation LHC IRs", *Proc. of EPAC 2002 Conf.*, Paris, pp. 2451-2453 (2002).

[13] S. Yadav and A.V. Zlobin, "Finite Element Analysis of the Effect of Cooling Conditions on Two-Layer and Four-Layer HGQ Magnet Designs", Fermilab Technical Report, TD-02-047 (2002).

[14] S. Yadav, V.V. Kashikhin, A.V. Zlobin, "Radiation Heating of an Nb_3Sn Cos-theta Separation Dipole", Fermilab Technical Report, TD-03-035 (2003).

[15] T. Sen et al., "Beam Physics Issues for a Possible 2nd Generation LHC IRs", *Proc. of EPAC 2002 Conf.*, Paris, pp. 371-373 (2002).

[16] P. Lebrun, *Cryogenics*, Supplement, Vol. 34, pp. 1-8 (1994).

[17] G. Passardi and L. Tavian, *Proc. 19th Intern. Cryo. Engn. Conf.*, Grenoble, France, pp. 53-58 (2002).

[18] T. Taylor , private communication (2003).